Electronic Supplementary Material (ESI) for Energy & Environmental Science.

SUPPORTING INFORMATION

The role of iodide on the formation of lithium hydroxide in lithium-oxygen batteries

M. Tułodziecki[*a], G. M. Leverick[b], C. V. Amanchukwu[c], Yu Katayama[b,d], D. G. Kwabi[b], Paula T. Hammond[c], Fanny Bardé[e] and Yang Shao-Horn[*a, b, f]

[a]Research Laboratory of Electronics, Massachusetts Institute of Technology, 77 Massachusetts Avenue, Cambridge, Massachusetts 02139, USA

[b]Department of Mechanical Engineering, Massachusetts Institute of Technology, 77 Massachusetts Avenue, Cambridge, Massachusetts 02139, USA

[c]Department of Chemical Engineering, Massachusetts Institute of Technology, 77 Massachusetts Avenue, Cambridge, Massachusetts 02139, USA

[d]Department of Energy Hydrocarbon Chemistry, Graduate School of Engineering, Kyoto University, Kyoto 615-8510, Japan

[e]Research & Development 3, Advanced Technology 1, Toyota motor Europe, Hage Wei 33 B, B-1930 Zaventem, Belgium

[f]Department of Materials Science and Engineering, Massachusetts Institute of Technology, 77 Massachusetts Avenue, Cambridge, Massachusetts 02139, USA

* Corresponding author: michalt@mit.edu, shaohorn@mit.edu

Key Words: Li-oxygen battery; Redox mediator; Discharge mechanism; Lithium iodide; Triiodide

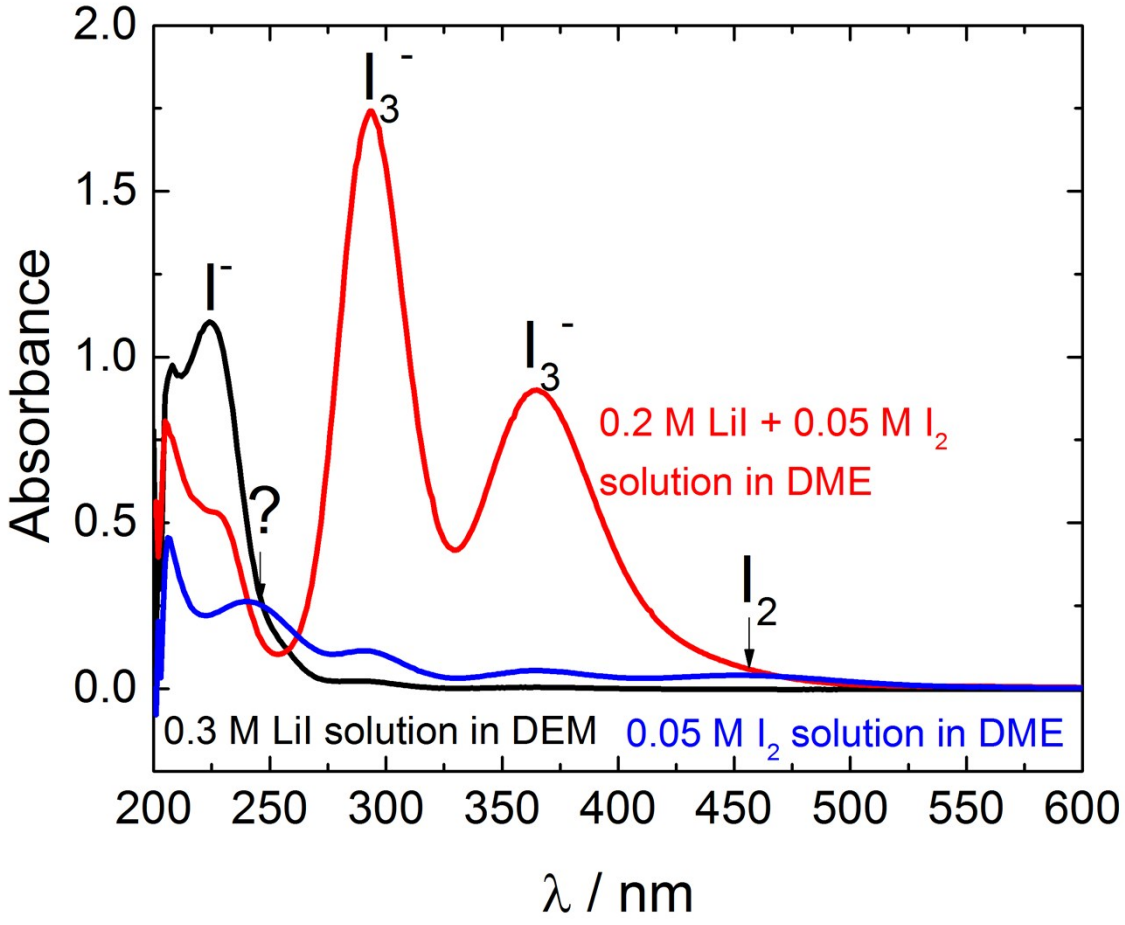

Figure S1. UV-Vis spectra of diluted stock solutions 0.3 M LiI – black curve, 0.2 M LiI + 0.0025 M I_2 – red curve and 0.05 M I_2 – blue curve. The spectra show the characteristic absorbance of I^- (223 nm), I_3^- (293 and 365 nm) and I_2 (245 nm, 451 nm). The observed peak at 240 nm for solution with I_2 is so far unidentified. It could be due to formation of either specific solvent–I^- or solvent–I^+ complexes.[1]

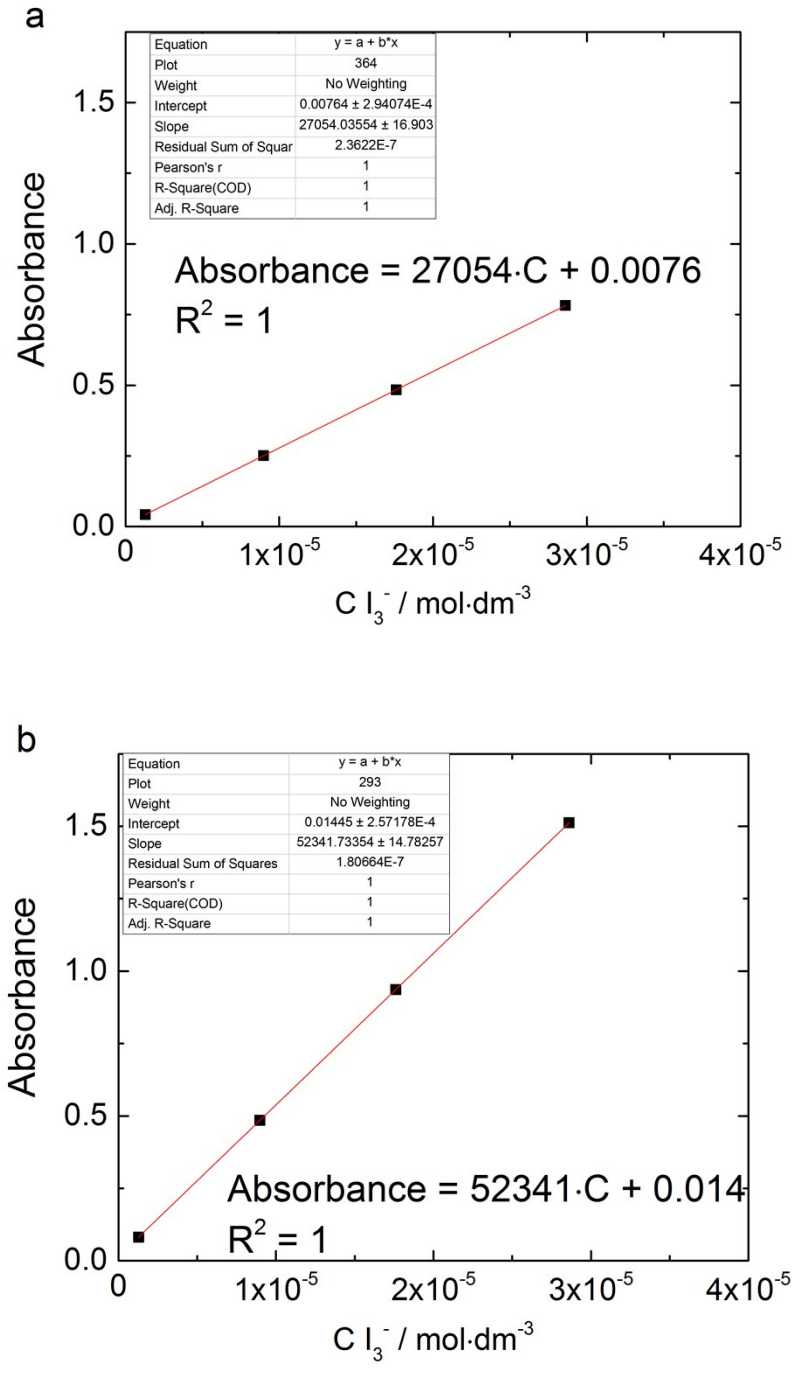

Figure S2 Calibration of I_3^- concentration done by measurement of different dilutions of stock solution 0.2 M LiI + 0.005M I_2 in DME a) signal at 364 nm b) signal at 293 nm

Table S1. Calculations of the triiodide concentration and the scale factor for figure plotting.

	sample	dilute 1	dilute 2	dilute 3	Absorption		^C I_3^- / mM	#Factor plotted / measured	Titration C I_3^- / mM
					293	364			
Figure 1	0.1M KO_2, 0.3 M LiTFSI, 40 ppm H_2O, 0.5 h	-	-	-	-	-	-	-	-
	0.1M KO_2, 0.3 M LiTFSI, 1000 ppm H_2O, 8 h	-	-	-	-	-	-	-	-
	0.1M KO_2, 0.2 M LiI, 0.1 M LiTFSI, 40 ppm H_2O, 0.5 h	100 µl + 3 ml DME	-	-	2.06	1.07	1.20 ± 0.01	0.05	1.2 ± 0.3
	0.1M KO_2, 0.2 M LiI, 0.1 M LiTFSI, 1000 ppm H_2O, 8 h	100 µl + 3 ml DME	100 µl + 3 ml DME	1 ml + 2ml DME	0.46	0.24	24.5 ± 0.8	2.1	24.4 ± 0.3
	0.1M KO_2, 0.2 M LiI, 0.1 M LiTFSI, 2000 ppm H_2O, 8 h	100 µl + 3 ml DME	100 µl + 3 ml DME	1 ml + 2ml DME	0.91	0.47	49 ± 1	2.1	49.3 ± 0.3
	0.1M KO_2, 0.2 M LiI, 0.1 M LiTFSI, 3000 ppm H_2O, 8 h	100 µl + 3 ml DME	100 µl + 3 ml DME	1 ml + 2ml DME	0.95	0.49	51 ± 2	2.1	50.6 ± 0.3
Figure 3a	0.3 M LiI, 40 ppm H_2O, Argon, 1 week	-	-	-	-	-	-	-	-
	0.3 M LiI, 40 ppm H_2O, Oxygen, 1 week	50 µl + 0.55 ml DME	-	-	1.46	0.76	0.312 ± 0.03	0.9	-
	0.3 M LiI, 1000 ppm H_2O, Oxygen, 1 week	100 µl + 1.0 ml DME	100 µl + 1.0 ml DME	-	0.62	0.32	0.95 ± 0.02	3	-
Figure 3b	0.1M KO_2, 0.3 M KI, 40 ppm H_2O, 2 days	300 µl + 0.55 ml DME	-	-	-	-	<0.01	1	-
	0.1M KO_2, 0.3 M KI, 1000 ppm H_2O, 2 days	100 µl + 0.55 ml DME	-	-	0.13	-	<0.01	1	-
Figure 3c	Li_2O_2, 0.3 M LiI, 40 ppm H_2O, 2 days	10 µl + 0.55 ml DME	-	-	0.70	0.36	0.729 ± 0.007	1	-
	Li_2O_2, 0.3 M LiI, 1000 ppm H_2O, 2 days	10 µl + 0.55 ml DME	-	-	0.97	0.51	1.03 ± 0.01	1	-
	Li_2O_2, 0.3 M LiI, 5000 ppm H_2O, 2 days	10 µl + 2.55 ml DME	-	-	0.74	0.38	3.57 ± 0.04	3.6	-

	sample	dilute 1	dilute 2	dilute 3	Absorption		^C I_3^- / mM	#Factor plotted / measured	Titration C I_3^- / mM
					293	364			
Figure 3d	0.1M KO_2, 0.3 M LiTFSI, 40 ppm H_2O + 0.2 M LiI, 0.5 h	100 µl + 3 ml DME	-	-	1.05	0.55	0.627 ± 0.006	0.2	0.6 ± 0.3
	0.1M KO_2, 0.3 M LiTFSI, 40 ppm H_2O + 0.2 M LiI, 16 h	100 µl + 1.55 ml DME	-	-	1.00	0.50	0.311 ± 0.003	-	-
	0.1M KO_2, 0.3 M LiTFSI, 1000 ppm H_2O + 0.2 M LiI, 24 h	100 µl + 3 ml DME	100 µl + 3 ml DME	-	1.25	0.64	23.0 ± 0.5	1	23.1 ± 0.3
Figure 5c	0.1M KO_2, 0.3 M LiI, H_2O:LiI = 0.25, H_2O:DME = 0.01, 24 h	50 µl + 3 ml DME	100 µl + 1 ml DME	0.5 ml + 3 ml DME	0.70	0.26	44 ± 1	-	-
	0.1M KO_2, 0.3 M LiI, H_2O:LiI = 0.50, H_2O:DME = 0.02, 24 h	50 µl + 3 ml DME	100 µl + 1 ml DME	0.5 ml + 3 ml DME	0.75	0.29	48 ± 1.5	-	-
	0.1M KO_2, 0.3 M LiI, H_2O:LiI = 1.00, H_2O:DME = 0.03, 24 h	50 µl + 3 ml DME	100 µl + 1 ml DME	0.5 ml + 3 ml DME	0.76	0.30	49 ± 1.5	-	-
	0.1M KO_2, 0.3 M LiI, H_2O:LiI = 2.00, H_2O:DME = 0.06, 24 h	50 µl + 3 ml DME	100 µl + 1 ml DME	0.5 ml + 3 ml DME	0.71	0.27	45 ± 1	-	-
	0.1M KO_2, 0.3 M LiI, H_2O:LiI = 5.00, H_2O:DME = 0.16, 24 h	50 µl + 1 ml DME	50 µl + 2.5 ml DME	-	0.80	0.32	12.4 ± 0.2	-	-
	0.1M KO_2, 0.3 M LiI, H_2O:LiI = 12.0, H_2O:DME = 0.40, 24 h	0.5 ml + 2 ml DME	-	-	0.61	0.32	0.06 ± 0.0006	-	-
	0.1M KO_2, 0.3 M LiI, H_2O:LiI = 24.0, H_2O:DME = 0.86, 24 h	1.5 ml + 1 ml DME	-	-	0.03	0.01	<0.0001	-	-

*Absorptions intensities at λ_1 = 293 nm and λ_2 = 364 nm. ^ Calculated concentration of I_3^- from the average of the two absorption bands unless one of the absorbance is out of calibration scale then only one wavelength was used. # Factor by which the measured data is scaled in order to visualize the difference in triiodide concentration in the manuscript figures. The I_3^- concentration error (determined from UV-Vis method) comes mostly from the pipetting procedure that varies depending on the number of dilutions and is estimated to 1%, 2% and 3% for 1, 2 and 3 dilutions, respectively. The I_3^- concentration error (determined from iodometric titration) is based on the burette tolerance of ±0.05 ml and equal to ±0.3 mM.

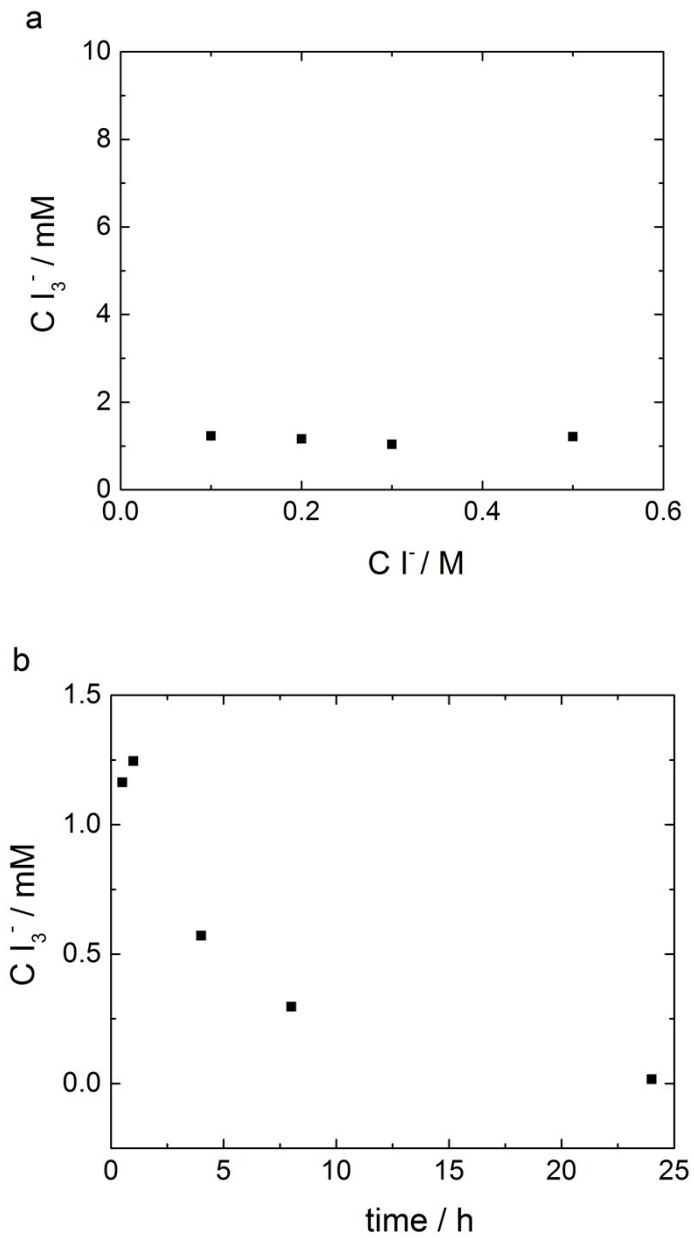

Figure S3. a) The LiI concentration dependence of I_3^- concentration after 30 min of reaction. The solutions tested where I) 0.1 M LiI + 0.2 M LiTFSI, II) 0.2 M LiI + 0.1 M LiTFSI, III) 0.3 M LiI and IV) 0.5 M LiI. b) The time dependence of I_3^- concentration in solution where 0.1 M KO_2 was directly added to 0.2 M LiI + 0.1 M LiTFSI solution in DME with 40 ppm H_2O. In all cases, the data is based on UV-Vis measurements only, as titration of the solutions with such small concentrations results in big errors. Each data point was obtained from separate new experiment.

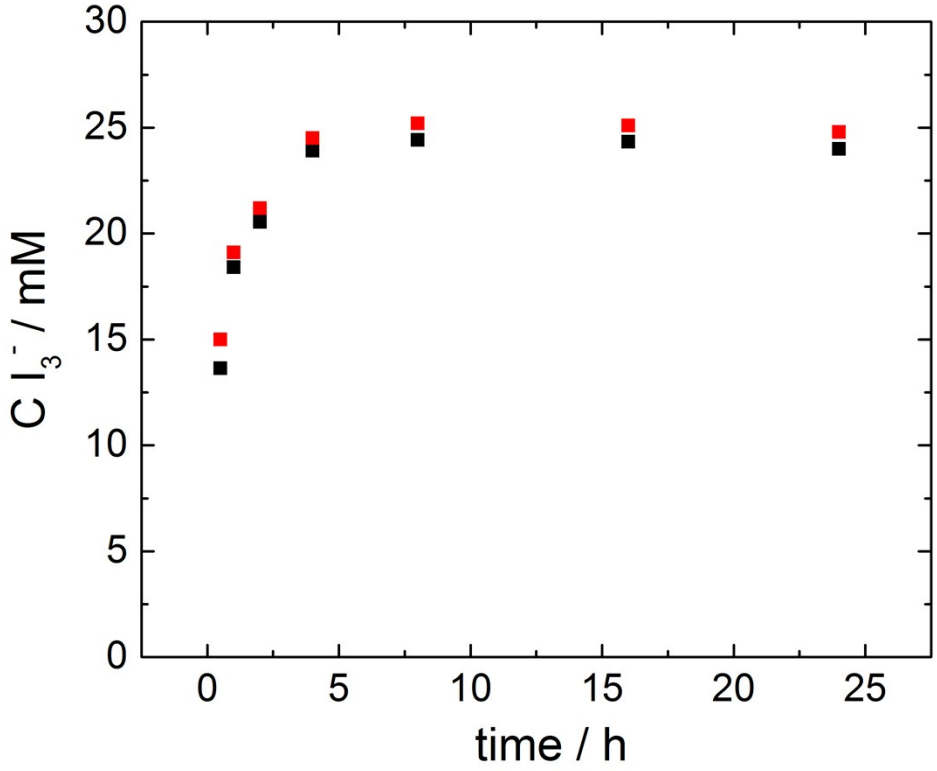

Figure S4. The time dependence of I_3^- concentration in solution where 0.1M KO_2 was directly added to 0.2 M LiI + 0.1 M LiTFSI solution in DME with 1000 ppm H_2O. Red squares correspond to values obtained from UV-Vis measurements, while black squares from iodometric titration. In general a good agreement between both techniques is observed. Each data point was obtained from separate new experiment.

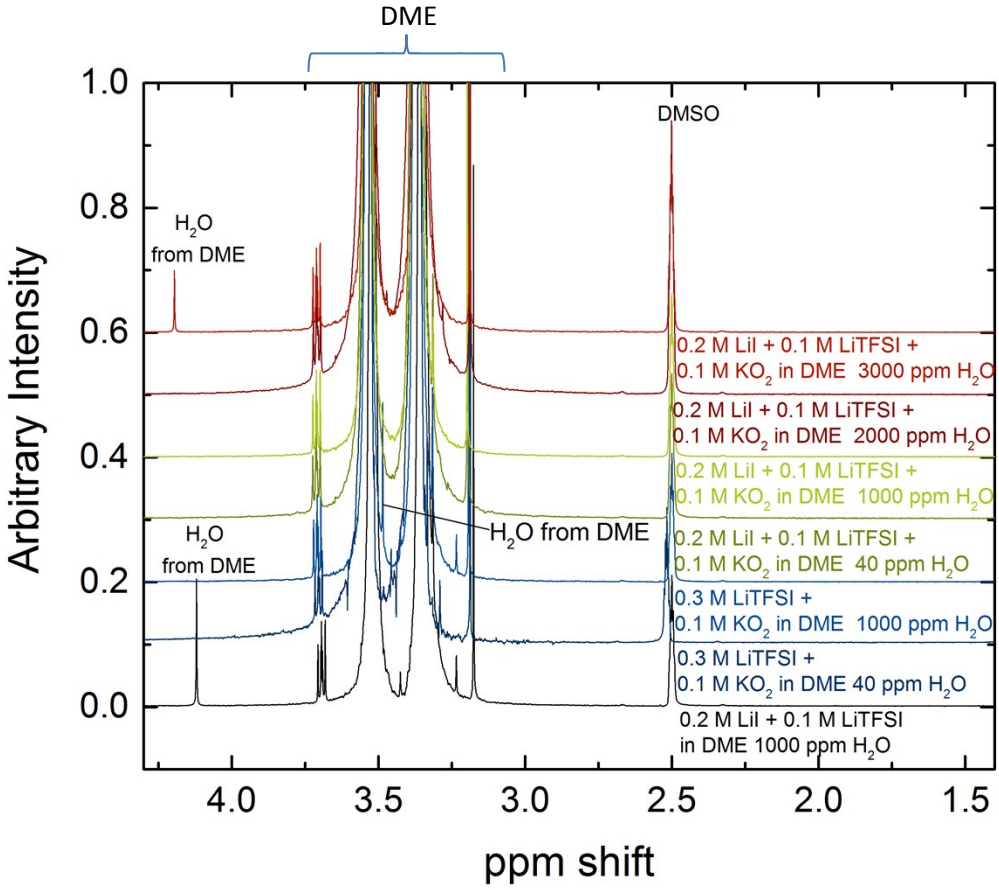

Figure S5 H^1NMR spectra of liquid phase from Figure 1. The spectra show no evidence for decomposition of DME. Moreover, the signal from H_2O (at ~4.2 ppm) disappeared after addition of KO_2 for all the samples containing LiI except the one containing 3000 ppm of H_2O (bright red). This confirms participation of H_2O in chemical processes during disproportionation reaction and formation of triiodide. For sample with 3000 ppm of H_2O no further increase of I_3^- was observed that corresponds to presence of unreacted H_2O and lack of Li_2O_2 phase. Sample with 1000 ppm H_2O and only LiTFSI salt (bright blue) showed also strong signal from H_2O at around 3.5 ppm, indicating lack of its consumption during disproportionation reaction. The shifts of the H_2O position are explained in the manuscript Figure 4a. The liquid part of sample was placed inside the capillary and closed with the Teflon cap. Next, the capillary was placed inside the NMR tube that contained the deuterated DMSO solvent. In such manner we avoid direct mixing of reference and sample solution, so that we can probe specific interactions between the species in the studied solution.

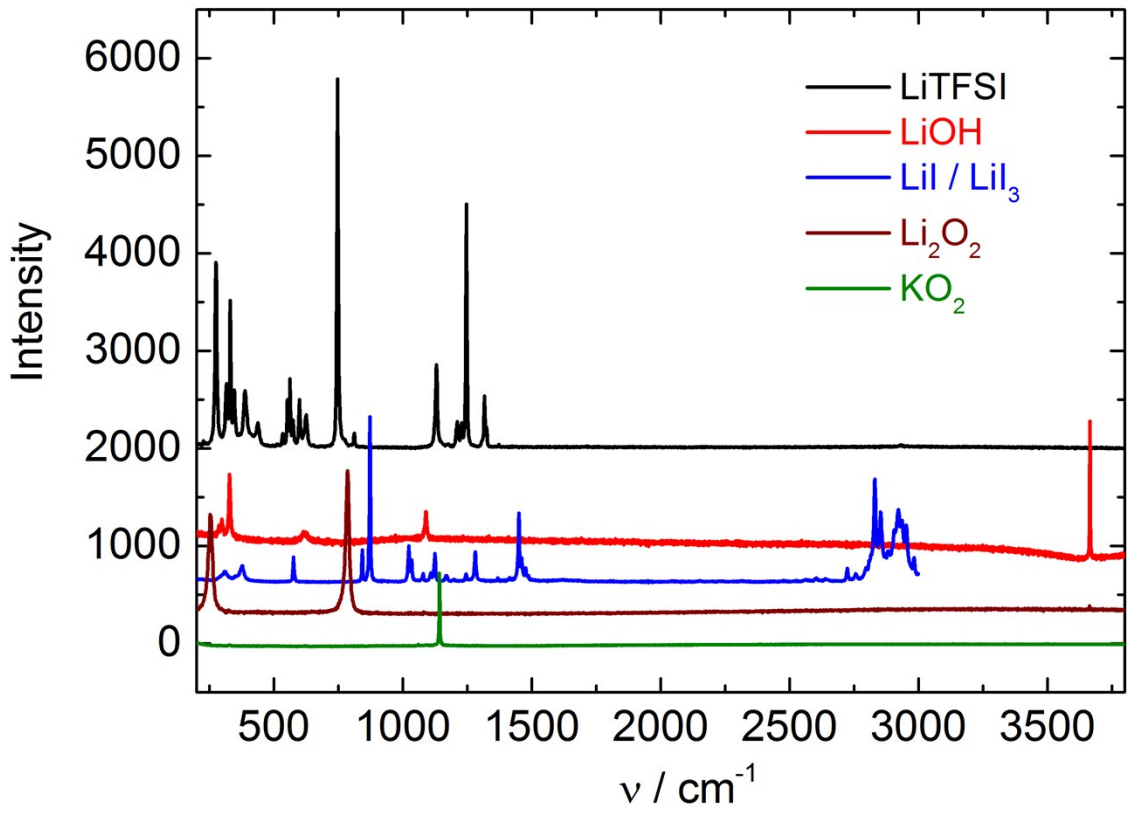

Figure S6. Reference Raman spectra of pure substances. In case of LiI powder, the spectra was evolving during the data acquisition due to oxidation of I^- by red laser. Pure LiI does not reveal any signal in the presented range, on the other hand I_3^- has multiple signals as seen on blue spectra.

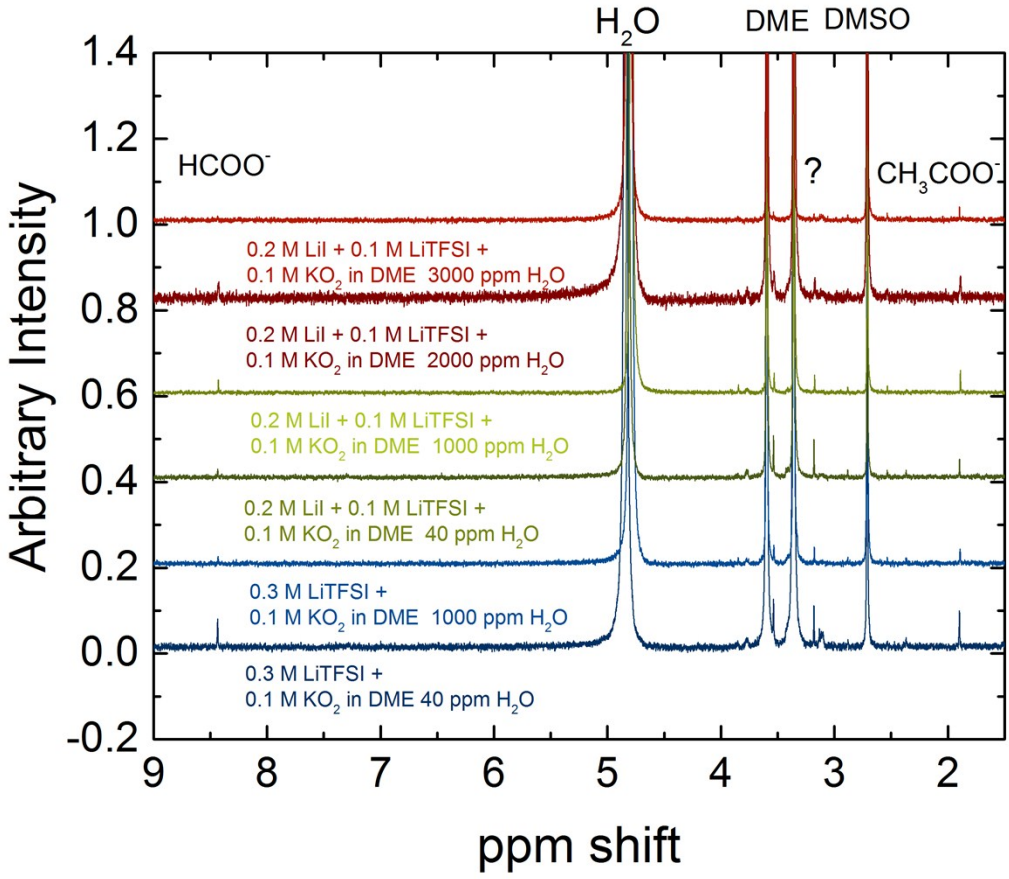

Figure S7 H^1NMR spectra of the solid phase from Figure 1. The spectra show tiny amounts of DME decomposition products $HCOO^-$ and CH_3COO^- at 8.5 ppm and 1.9 ppm shifts. The concentration of the decomposition products in the solution for H^1NMR analysis was around 0.1-0.2 mM (considering 3mM concentration of DMSO) that corresponds to 0.1-0.2 mM concentration in the reaction solution as the same volumes of the solutions were used. Signal at 4.9 ppm corresponds to H_2O. 2 Strong signals at 3.4 and 3.6 ppm correspond to residual DME. Signal at 2.7 ppm corresponds to DMSO. Small signals at 3.2 ppm could not be identified, however it probably comes from initial impurities of DME as such signals were present in the pristine solution, Figure S5 black curve. The solid part was first dissolved in D_2O solution with added known amount of DMSO (3 mM) for quantification purpose. The resulted solution was directly placed in the NMR tube (no capillary).

Detailed description on the possibilities of I^- oxidation

Iodide can be oxidized to triiodide by peroxy like species as hydrogen peroxide[2] or hydroperoxy anion, reactions 1-4[3].

$$H_2O_2 + I^- \rightarrow IO^- + H_2O \quad (1)$$

$$IO^- + 2I^- + H_2O \rightarrow I_3^- + 2OH^- \quad (2)$$

$$HO_2^- + I^- \rightarrow IO^- + OH^- \quad (3)$$

$$IO^- + 2I^- + H_2O \rightarrow I_3^- + 2OH^- \quad (4)$$

In fact, iodide is used as an indicator of H_2O_2 due to the high absorption coefficient of triiodide that allows detection of trace H_2O_2 (0.05 mg/dm^3)[2]. Indeed H_2O_2 species in absence of iodide where detected by the quantofix stripes at concentration of 2 mg/L. Formation of hydrogen peroxide and its related species can occur in few different reaction paths in Li-air battery:

i) superoxide ion reaction[4-7] with water[7] or ether based solvent[4] (proton source), reaction 5-7

$$O_2^- + H^+_{H2O \text{ or } DME} \rightarrow HOO^* \quad (5)$$

$$HOO^* + O_2^- \rightarrow HOO^- + O_2 \quad (6)$$

$$Li^+ + HOO^- + H_2O \rightarrow LiOH + H_2O_2 \quad (7)$$

ii) lithium peroxide reaction with water[7] or ether based solvent[8-10], reaction 8-9

$$Li_2O_2 + 2H_2O \leftrightarrow 2LiOH + H_2O_2 \quad (8)$$

$$Li_2O_2 + CH_3O\text{-}R_1 \leftrightarrow CH_3OLi + R_2 + HOO^-Li^+ \quad (9)$$

and iii) O_2 reaction with ether based solvent, reaction 10-11[4, 6, 11].

$$RH + O_2 \rightarrow R^* + HOO^* \quad (10)$$

$$RH + HOO^* \rightarrow R^* + H_2O_2 \quad (11)$$

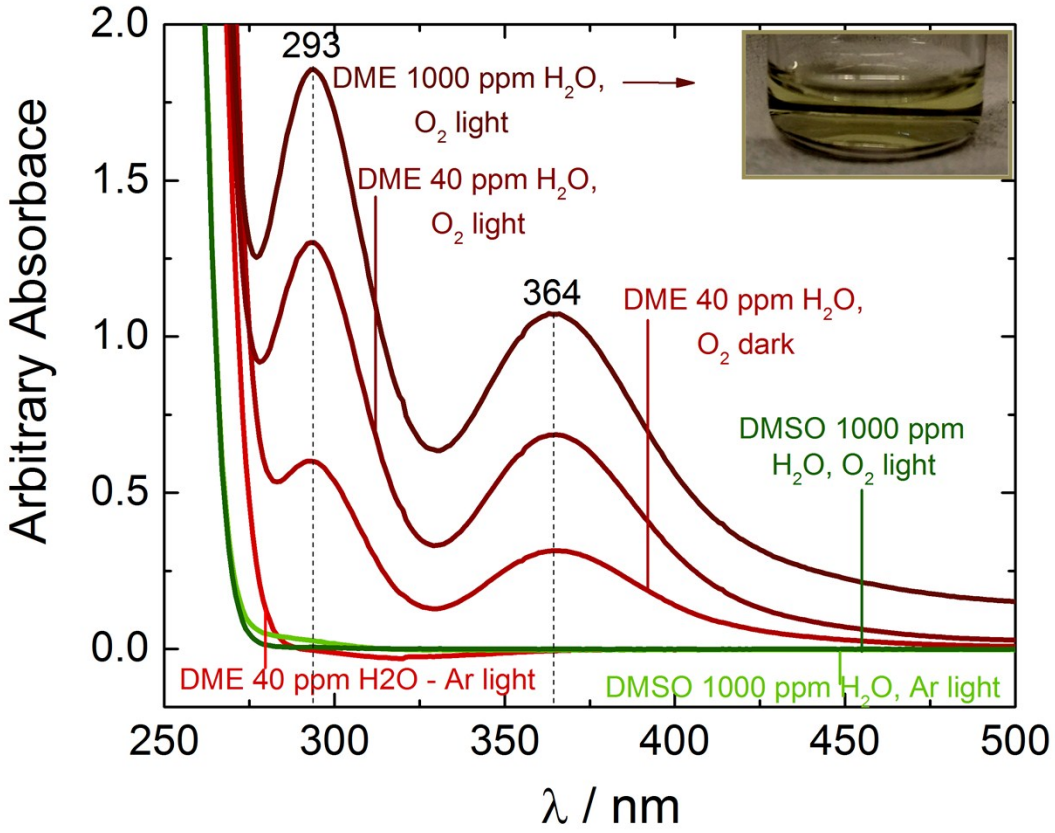

Figure S8. The influence of oxygen, light, and water on the stability of I^- in solution. UV-Vis spectra of 0.3 M LiI solutions in DME and DMSO. The spectra are taken after 1 week of storage in defined conditions.

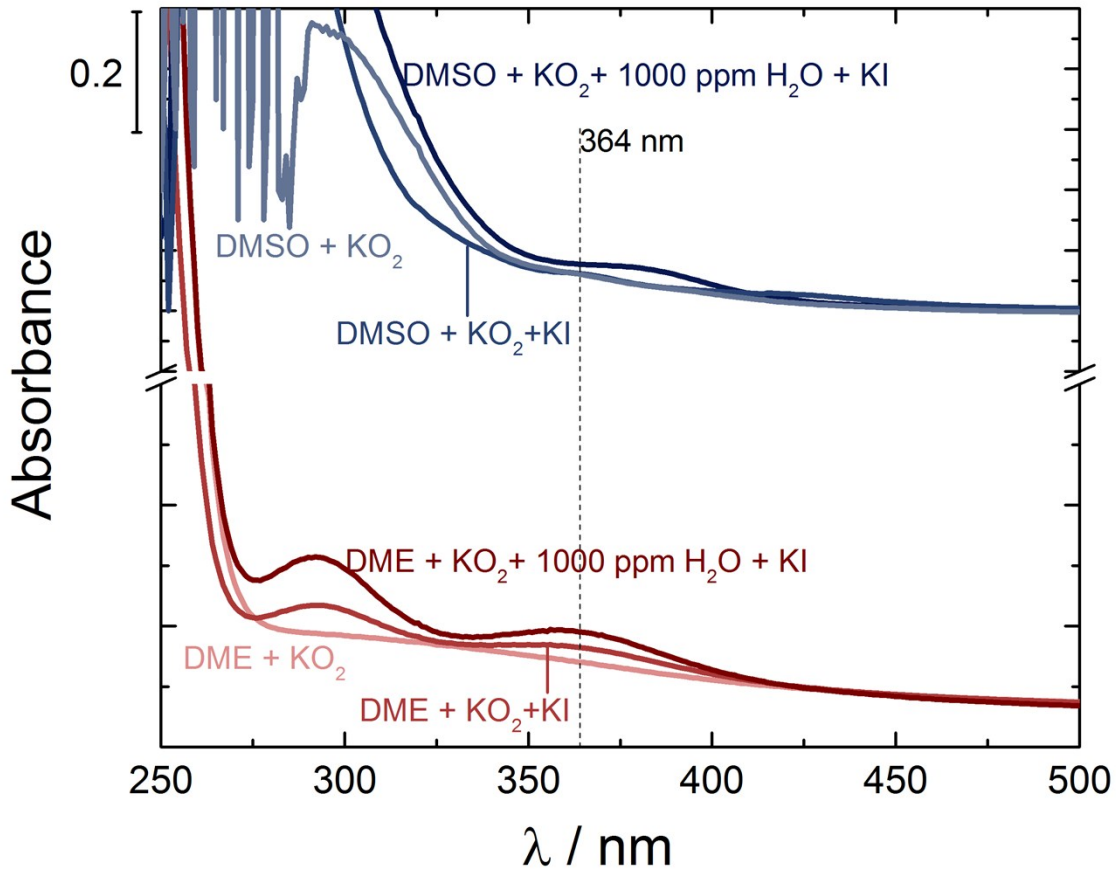

Figure S9. UV-Vis spectra of DME (bottom) and DMSO (top) solutions containing KO_2 after 2 days. Calculation of the I_3^- concentration from absorption values at 293 nm and 364 nm was done after subtraction of the reference DME + KO_2 spectra to avoid contribution from O_2^- absorption. Only small fraction of the added KO2 is soluble in the electrolyte, which is higher for DMSO as compare to DME.

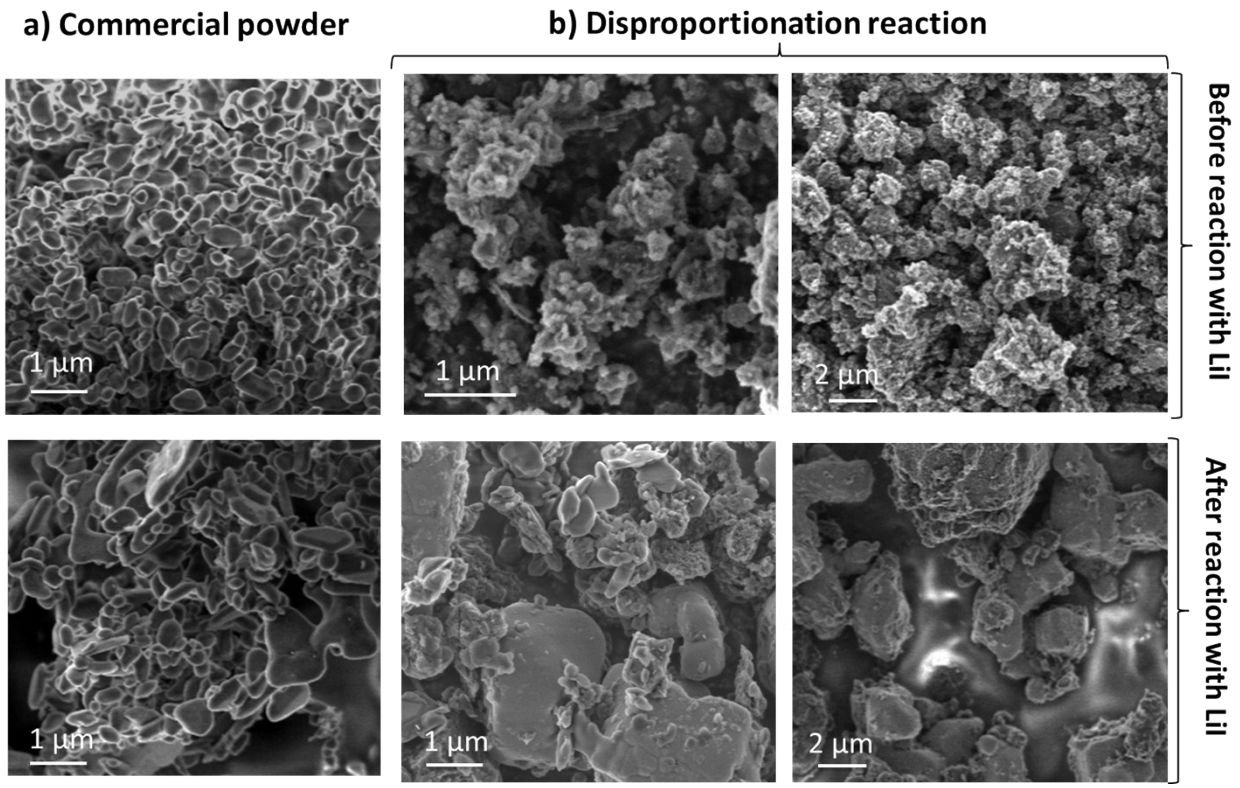

Figure S10 SEM images of a) commercial Li_2O_2 and b) Li_2O_2 from disproportionation reaction before (top) and after reaction with LiI (bottom).

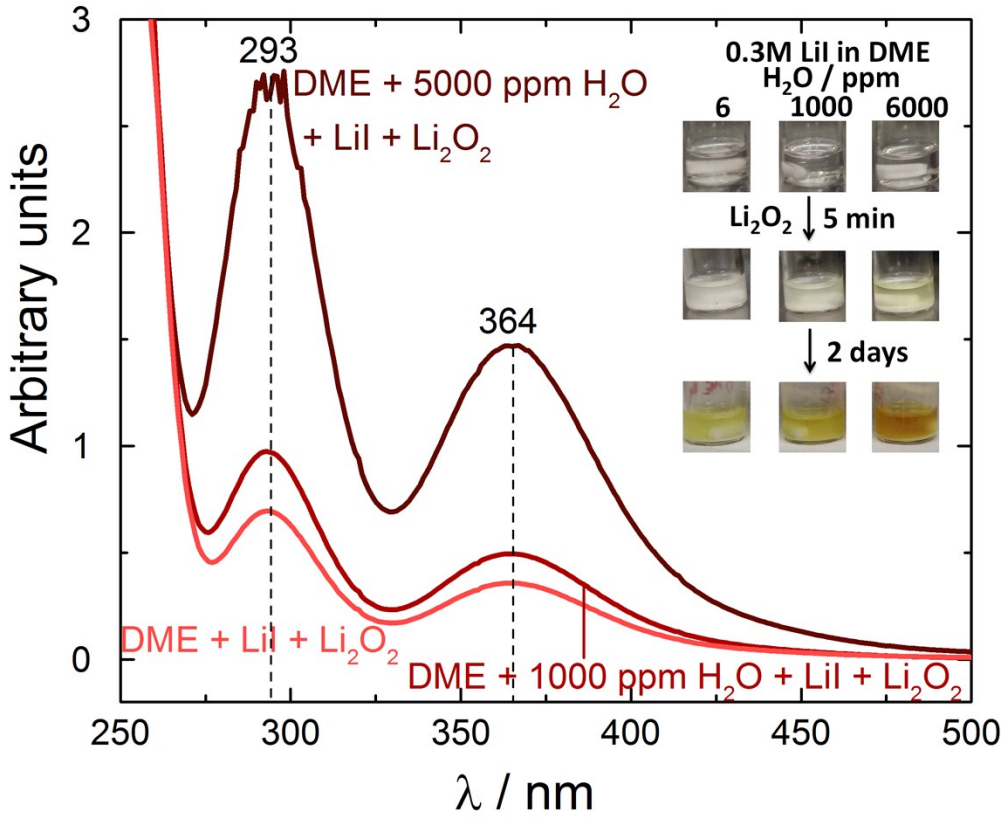

Figure S11. The UV-Vis spectra of 0.3 M LiI mixed with commercial Li_2O_2 powder (0.1 g) in DME with 40, 1000 and 5000 ppm H_2O after 2 days. The inset shows optical photographs of the mixture after 5 minutes and 2 days.

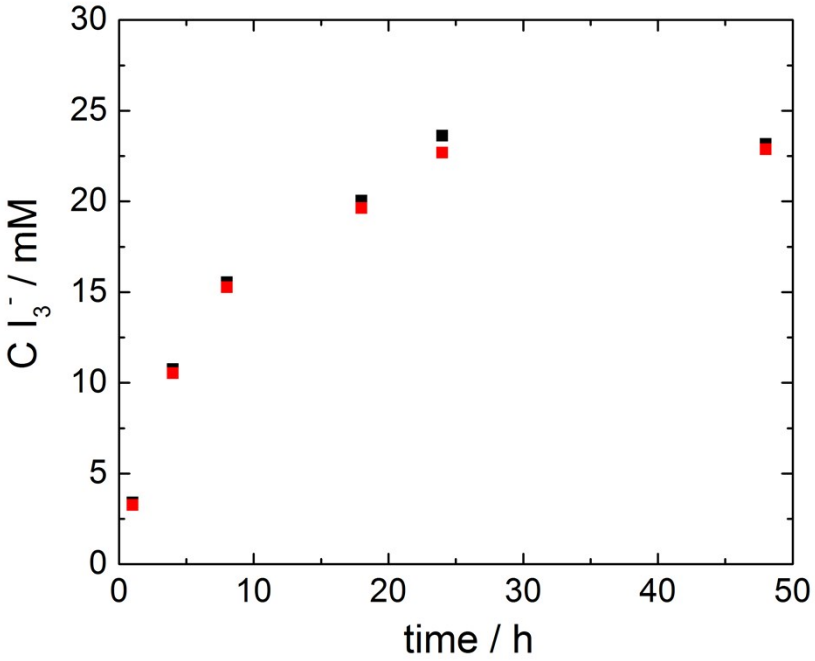

Figure S12. The time dependence of I_3^- concentration in solution where 0.2 M KO_2 was first added to 0.6 M LiTFSI solution and after 20 min 0.4 M LiI solution was added. The final concentrations of Li salt after mixing the two solutions were 0.3 M LiTFSI and 0.2 M LiI. Both solutions were prepared with DME containing 1000 ppm of H_2O. Red squares correspond to values obtained from UV-Vis measurements, while black squares from iodometric titration. In general a good agreement between both techniques is observed. Each data point was obtained from separate new experiment.

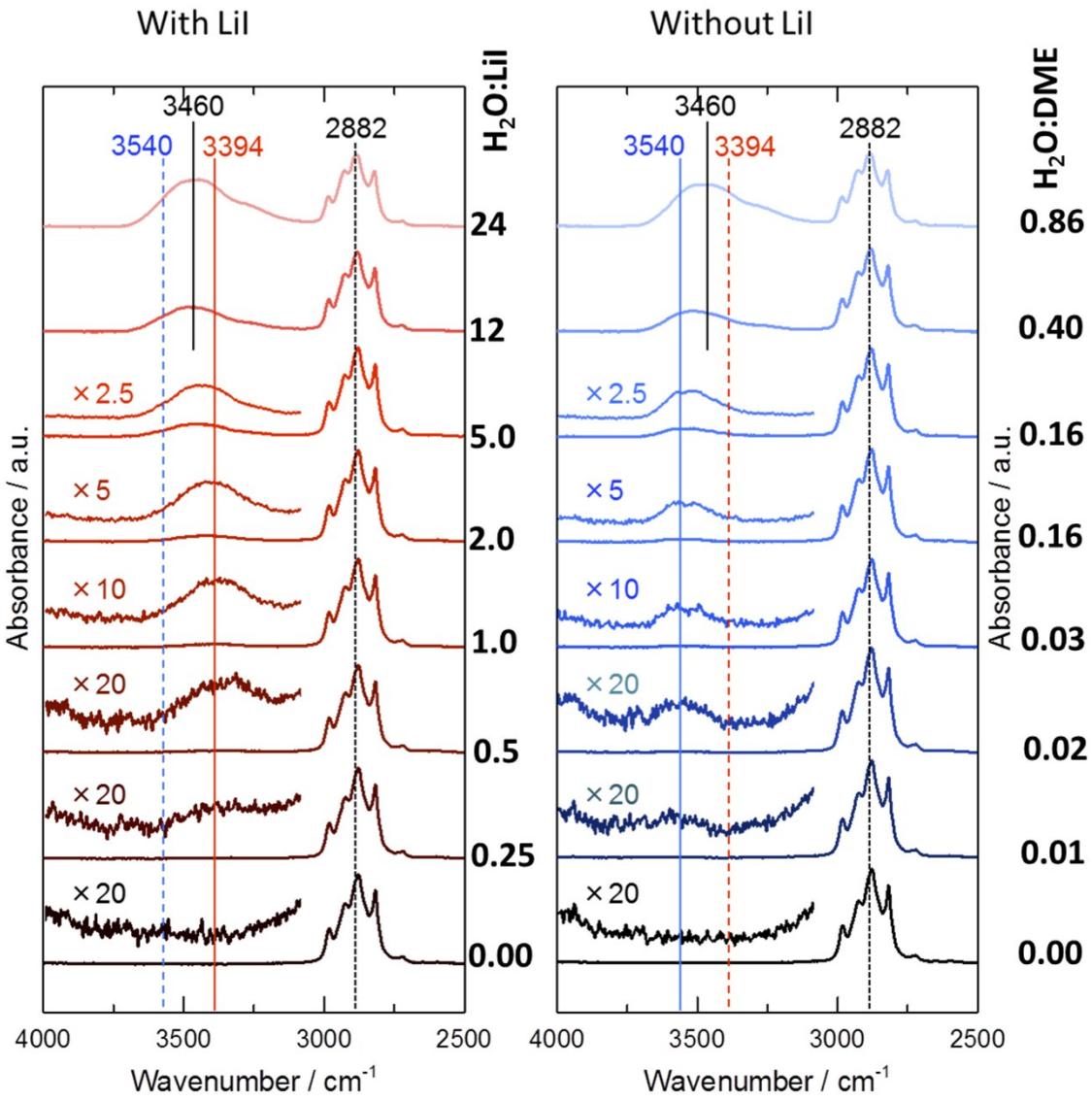

Figure S13. The FT-IR spectra of pure DME and 0.3 M LiI solution in DME with different H_2O content.

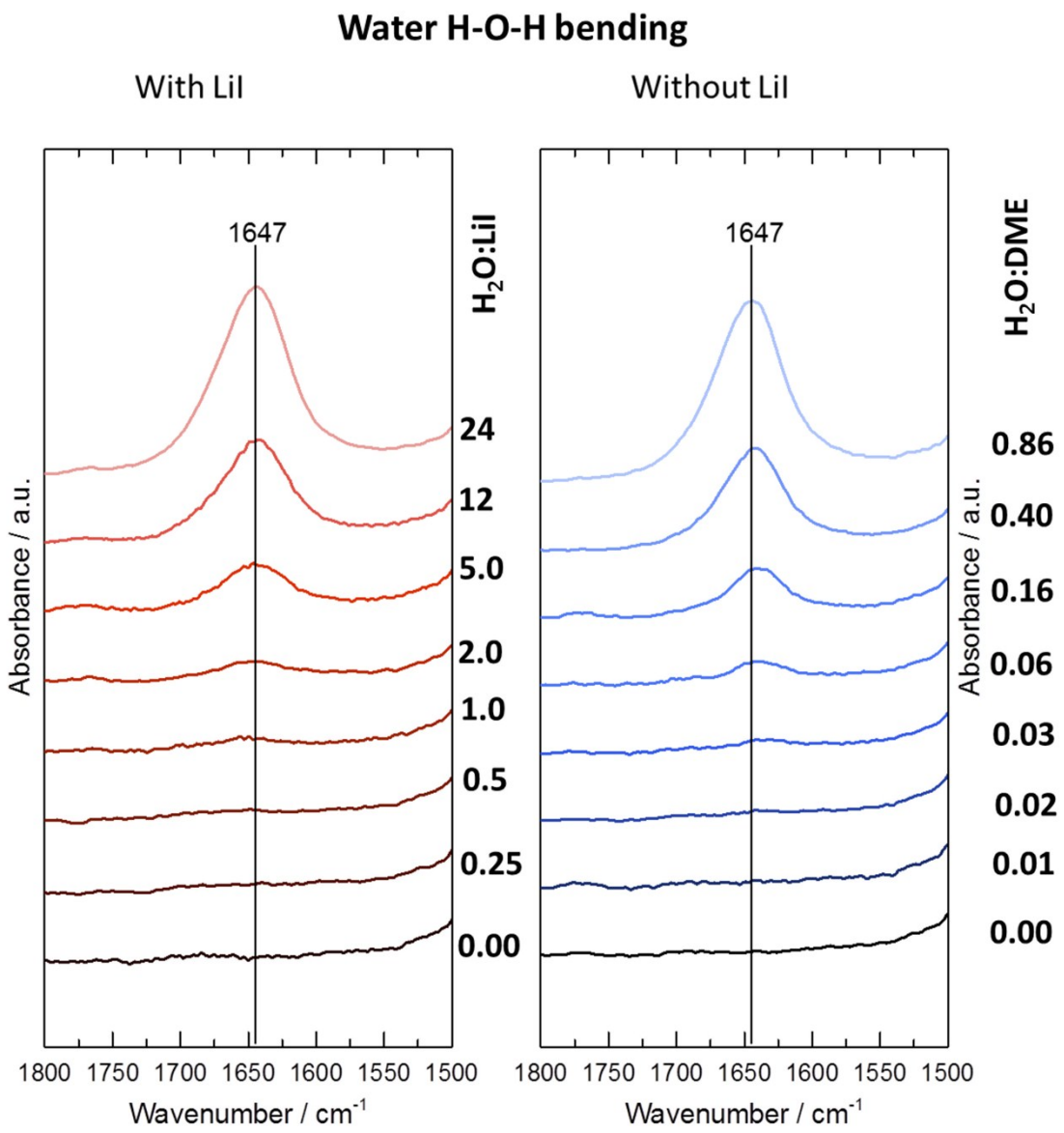

Figure S14. The FT-IR spectra of pure DME and 0.3 M LiI solution in DME with different H_2O content showing the region of water bending vibration.

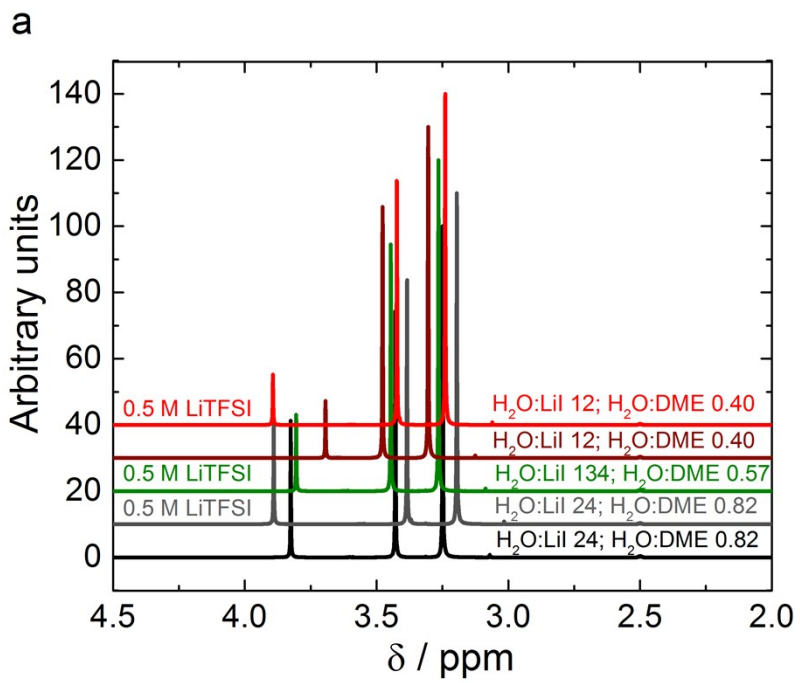

Figure S15. a) 1HNMR spectra of the pristine electrolytes used to perform disproportionation reaction.

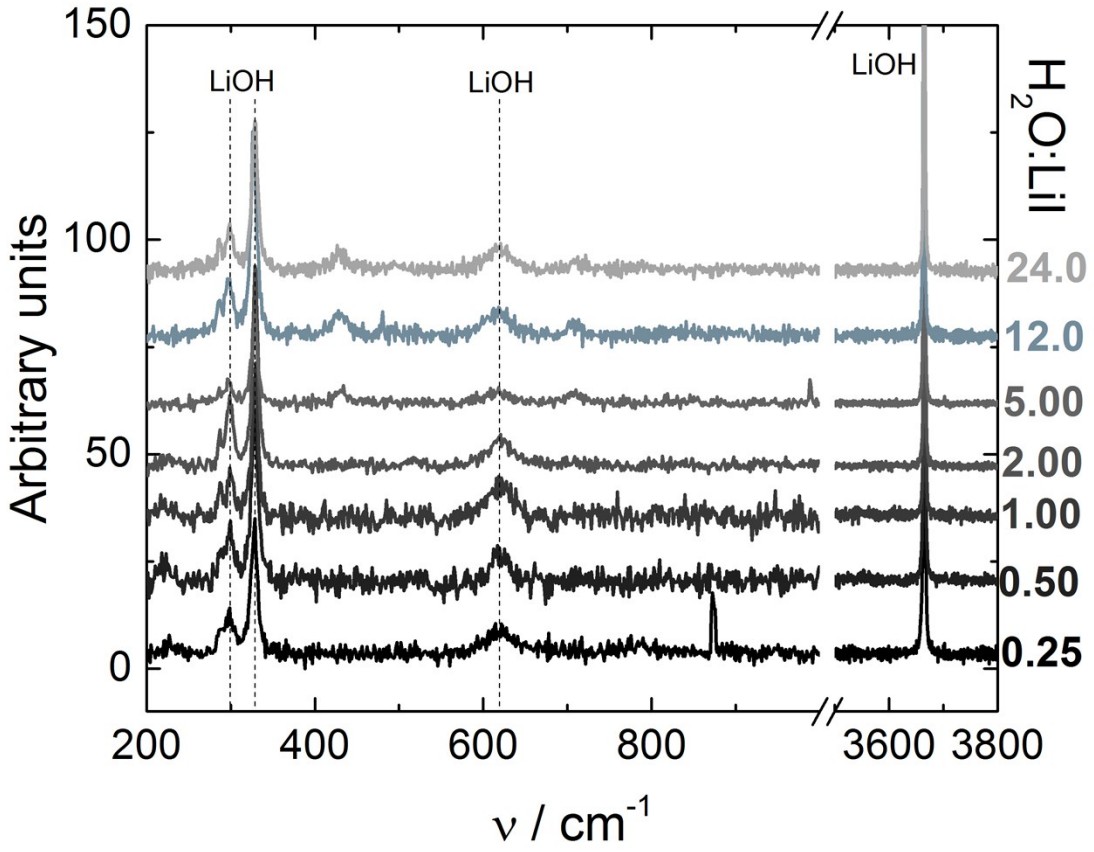

Figure S16 Raman spectra of powders obtained from LiO_2 disproportionation reaction (0.3 M LiI + 0.1 M KO_2 24 h) in different H_2O:DME ratios (The LiI:H_2O ratio indicated on the right) with reaction time 24 h, the powders were washed 3 times with anhydrous DME before the experiment. The coloring scheme is consistent with Figure 5 a, b.

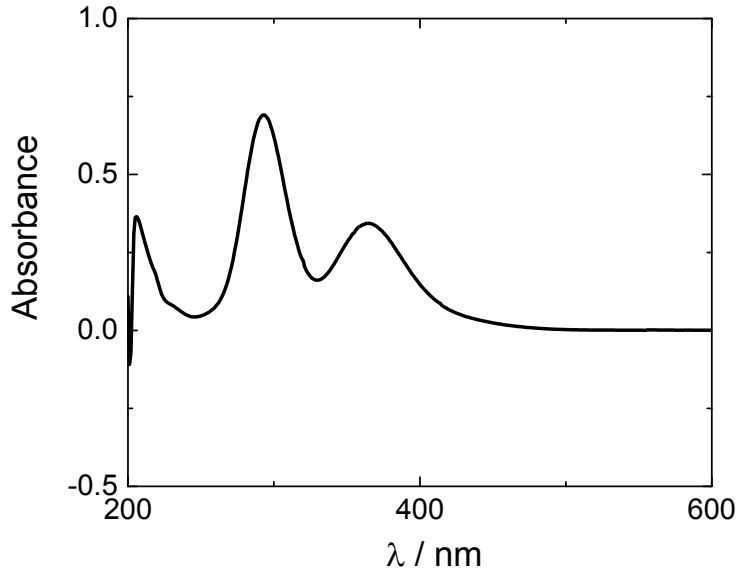

Figure S17. The UV-Vis of diluted electrolyte (0.1M LiI + 0.2M LiTFSI in DME with 1000 ppm H_2O) coming from discharged battery at 2.7 V.

1. Z. Kebede and S.-E. Lindquist, *Sol. Energ. Mat. Sol. Cells*, 1999, **57**, 259-275.
2. P. J. Brandhuber and G. Korshin, *Methods for the detection of residual concentrations of hydrogen peroxide in advanced oxidation process*, Watereuse Foundation, Alexandria, 2009.
3. M. C. Milenkovic and D. R. Stanisavljev, *Russ. J. Phys. Chem. A*, 2011, **85**, 2279-2282.
4. B. D. Adams, R. Black, Z. Williams, R. Fernandes, M. Cuisinier, E. J. Berg, P. Novak, G. K. Murphy and L. F. Nazar, *Adv. Energy Mater.*, 2015, **5**, 1400867.
5. Y. Che, M. Tsushima, F. Matsumoto, T. Okajima, K. Tokuda and T. Ohsaka, *J. Phys. Chem.*, 1996, **100**, 20134-20137.
6. V. S. Bryantsev and F. Faglioni, *J. Phys. Chem. A*, 2012, **116**, 7128-7138.
7. D. G. Kwabi, T. P. Batcho, S. Feng, L. Giordano, C. V. Thompson and Y. Shao-Horn, *Phys. Chem. Chem. Phys.*, 2016, **18**, 24944-24953.
8. W. J. Kwak, D. Hirshberg, D. Sharon, H. J. Shin, M. Afri, J. B. Park, A. Garsuch, F. F. Chesneau, A. A. Frimer, D. Aurbach and Y. K. Sun, *J. Mater. Chem. A*, 2015, **3**, 8855-8864.
9. D. Sharon, V. Etacheri, A. Garsuch, M. Afri, A. A. Frimer and D. Aurbach, *J. Phys. Chem. Lett.*, 2013, **4**, 127-131.
10. D. Sharon, M. Afri, M. Noked, A. Garsuch, A. A. Frimer and D. Aurbach, *J. Phys. Chem. Lett.*, 2013, **4**, 3115-3119.
11. S. Di Tommaso, P. Rotureau, O. Crescenzi and C. Adamo, *Phys. Chem. Chem. Phys.*, 2011, **13**, 14636-14645.